ISSN 1023-1935, Russian Journal of Electrochemistry, 2013, Vol. 49, No. 6, pp. 545–556. © Pleiades Publishing, Ltd., 2013.
Original Russian Text © Yu.G. Chirkov, V.I. Rostokin, A.M. Skundin, 2013, published in Elektrokhimiya, 2013, Vol. 49, No. 6, pp. 614–626.

Lithium Ion Rechargeable Battery, Galvanostatics: Computer Simulation and Calculation of Characteristics of the Active Layer of Arbitrary Thickness with Low Lithium Atom Diffusivity

Yu. G. Chirkov[a, z], V. I. Rostokin[b], and A. M. Skundin[a]

[a] *Frumkin Institute of Physical Chemistry and Electrochemistry, Russian Academy of Sciences, Leninskii pr. 31, Moscow, 119071 Russia*

[b] *National Research Institute of Nuclear Energy, Russia*

Received March 11, 2012

Abstract—The work of a lithium ion rechargeable battery operating under galvanostatic discharge conditions is simulated. Attention is focused on the complete mathematical description of processes in electrode active layers. The central problem in the theory of lithium ion batteries is the possibility of analyzing the following two processes that proceed simultaneously in space and time: depletion and enrichment of the active substance (intercalator) grains with lithium atoms and the ohmic-limitation-induced redistribution of the electrode potential in time throughout the active layer thickness. A new approach to the central problem is considered. It is based on comparing the characteristic times of two main processes occurring in electrodes. Here, the lithium atom diffusivity in intercalator grains plays the decisive role. Two regions of diffusivity values, i.e., high and low, can be singled out. Algorithms are developed for solving the complete system of equations for the most complicated case, namely, active layers of arbitrary thickness with low diffusivity of lithium atoms. The following electrode working parameters (for anode) are calculated: optimal active layer thickness, discharge time, anode specific capacitance, and final potential at the active layer/interelectrode space interface.

Key words: lithium ion battery, galvanostatics, computer simulation of active layers, model of equal-sized cubic grains, regions of high and low diffusivity of lithium atoms, calculation of working parameters for anodes with the active layer of arbitrary thickness and a low lithium atom diffusivity.

DOI: 10.1134/S1023193513060025

1. FORMULATION OF THE PROBLEM

As was shown in [1, 2], the computer simulation of active layers of lithium-ion battery electrodes includes several steps. It is necessary to (1) develop the model of a porous electrode, (2) study the percolation properties of this model, (3) determine the effective coefficients of the active layer, (3) write a system of equations describing the totality of processes in the active layer, (5) estimate the following working parameters of the active layer: the optimal thickness of the active layer, the discharge time, the specific capacitance, and the final potential at the active layer/interelectrode space interface.

In most cases, the electrode active layer of a lithium ion battery represents a system with doubly distributed parameters. In commercial lithium-ion batteries, the active layer of negative electrodes consists of particles of a carbon material (capable of reversible lithium intercalation) with liquid or polymer electrolyte in between. On its back side, the active layer adjusts a current collector; its front side faces the electrolyte. At the discharge of such electrode, lithium ions move in pores from the front side to the back side; their discharge takes place at the interface of a carbon particle with electrolyte and the resulting lithium atom moves inside the particle by the solid-state diffusion mechanism. Thus, to describe the charging process, it is necessary to take into account the ion transport in electrolyte (i.e., the electrolyte conductivity), the discharge process (i.e., the kinetics of the electrochemical process as such), and the solid-phase diffusion. The electrolyte conductivity is usually known. The discharge kinetics is still much unclear being usually described by a formal equation of slow discharge with empirical exchange current. The exchange current density on a particle into which lithium ions are being incorporated depends on the surface concentration of lithium in this particle and in electrolyte. For graphite with the degree of intercalation close to 0.5, the exchange current density is assumed to be from 0.04 mA/cm^2 [3] to 40 mA/cm^2 [4]. The literature data on the diffusivity are discrepant: for different carbon materials, its values vary from 10^{-12} to $10^{-6.4}$ cm^2/s [5]. Such a wide scatter is determined first of all by the difference in the nature of carbon materials studied in different works

[z] Corresponding author: olga.nedelina@gmail.com (Yu.G. Chirkov).

and also by the dependence of diffusivity on the potential observed in many studies. Experimental data for other negative electrodes materials are scarce. In the literature, one can find descriptions of materials with rather high or very low diffusivities. The first group includes, for example, tin, zinc, and cadmium for which the lithium diffusivity is from 10^{-9} to 10^{-7} cm^2/s [6–8] or cobalt oxides with the lithium diffusivity of 10^{-9}–10^{-8} cm^2/s [9–10]. The second group includes amorphous silicon with lithium diffusivity from 10^{-13} to 10^{-12} cm^2/c [11–14], tin borophosphate ($Sn_2BP_{1-x}Sb_xO_6$ $0 < x < 0.3$) with lithium diffusivity of $(0.3–3.5) \times 10^{-14}$ cm^2/s [15], nanocrystalline $CeO_{2-\delta}$ (lithium diffusivity about 10^{-15} cm^2/s) [16], nanocrystalline $CdSnO_3$ (lithium diffusivity of $(0.1–3.5) \times 10^{-13}$ cm^2/s [17], Co_3O_4 doped with ZrO_2 (lithium diffusivity 3×10^{-14} cm^2/s [18].

This study is aimed at elaborating algorithms of computations which would allow us to efficiently assess the parameters of active layers of electrode for lithium-ion batteries containing materials with low lithium diffusivity and also to demonstrate examples of calculations of working parameters.

2. SYSTEM OF EQUATIONS FOR THE ELECTRODE ACTIVE LAYER

First of all, we present a system of equations describing the spatial and temporal behavior of processes that occur in the electrode active layer within a lithium ion battery. Below, we will discuss anodes bearing in mind that the processes on the cathode are of the similar nature.

The normalized average lithium concentration in intercalator grains is $\check{c} = c/c^*$, where c^* is the maximum possible concentration of lithium atoms. In the initial moment (at $t = 0$), all intercalator grains are filled with lithium atoms up to concentration $\check{c} = c_0$; later, at the anode discharge, the concentration of lithium atoms begins to decrease.

The current density j generated at the boundary of ionic (the aggregate of interconnected electrolyte grains) and electronic (the aggregate of interconnected intercalator grains) percolation clusters is as follows:

$$j = i_0[(1-a_s)^{1/2}a_s^{1/2}]\{e^{\eta} - e^{-\eta}\}, \quad (1)$$

where a_s is the normalized concentration of lithium atoms in active intercalator grain at the surface of their contact with electrolyte grains involved in the ionic percolation cluster, i_0 is the exchange current. The normalized electrode polarization is

$$\eta = F[E-U]/2RT, \quad (2)$$

where E is the electrode potential. For the sake of definiteness, we assume that the potential U at the open circuit [13] is as follows:

$$U = -0.16 + 1.32\exp(-3\check{c}). \quad (3)$$

For anode, we can assume that the concentration of lithium ions in intercalator active grains is confined within the limits $0.0 < \check{c} < c_0 = 0.7$ [3].

Based on the law of conservation of lithium ion flows in electrolyte (in grains of the ionic percolation cluster), we can find the equation for polarization η in the electrode active layer

$$d^2\eta/d\hat{y}^2 = [(1-a_s)^{1/2}a_s^{1/2}]\{e^{\eta} - e^{-\eta}\}, \quad (4)$$

where $\hat{y} = y/L_{ohm}$ is the normalized coordinate, L_{ohm} is the characteristic ohmic length

$$L_{ohm} = (2RTk^*k/FSi_0)^{1/2}, \quad (5)$$

Here, k is the specific conductivity of electrolyte, k^* is the conductivity of lithium ions in the ionic percolation cluster (dimensionless value; the product $k\,k^*$ is the effective electrolyte conductivity in the anode active layer), S is the specific surface of contact between electronic and ionic percolation clusters; electrochemical reactions occur on this surface. The boundary conditions for Eq. (4) that describes the electrode discharge in the galvanostatic mode are as follows:

$$-I_{ohm}d\eta/d\hat{y} = I = \text{const} \quad \text{при } y = 0, \quad (6)$$

$$d\eta/d\hat{y} = 0 \quad \text{при } y = \Delta, \quad (7)$$

where Δ is the electrode active layer thickness, I is the discharge current density, and the characteristic ohmic current is

$$I_{ohm} = (2RTk^*kSi_0/F)^{1/2}. \quad (8)$$

The process of a depletion of intercalator active grains of lithium atoms is described by the equation

$$d\check{c}/dt^{**} = -[(1-a_s)^{1/2}a_s^{1/2}]\{e^{\eta} - e^{-\eta}\} = -j/i_0, \quad (9)$$

in which $\check{c}(y, t)$ is the concentration of lithium atoms averaged over the intercalator grain in moment t in the anode active layer section with coordinate y. The normalized current value of the discharge time t^{**} is as follows:

$$t^{**} = t/\tau, \quad (10)$$

Here, τ is the characteristic discharge time determined by the expression

$$\tau = g^*Fc^*/Si_0, \quad (11)$$

where g^* is the fraction of intercalator grains in the active layer. The initial condition for Eq. (9) is

$$\check{c} = c_0 \quad \text{при } t = 0. \quad (12)$$

Thus, the combination of Eqs. (4) and (9) together with boundary and initial conditions seemingly makes

it possible to follow the changes in time and in each point of the electrode active layer of the normalized potential

$$\psi = FE/2RT, \quad (13)$$

and the concentration of lithium atoms $\check{c}$ averaged over the volume of intercalator active grains. However, this can be done only if we know the concentration of lithium atoms a_s involved in the right sides of Eqs. (4) and (9). Thus, the system of equations (4) and (9) appears to be incomplete. It is necessary to specify the relationship between a_s and $\check{c}$. Thus, we have to consider the problem of diffusion limitations in intercalator active grains.

3. INTERCALATOR ACTIVE GRAIN

It was demonstrated [9] that the model of equal-sized cubic grains of two types (the anodic active layer of a lithium-ion battery) assumes that the real contribution to the electrochemical process is made by only a part of the external surface of intercalator active grains. Moreover, the distribution of electrochemically active regions over the in active grain external surface is rather complicated.

A simplified model of the intercalator active grain structure and the diffusion process at discharge in this grain was proposed [19]. The real diffusion process of lithium atoms was demonstrated to be three-dimensional rather than quasi-one-dimensional.

According to the model of an intercalator active grain proposed in [19], the distribution of lithium atom concentration $a = c/c^*$ along coordinate x in the active grain satisfies the equation

$$da/dt^* = d^2a/dz^2, \quad (14)$$

where z is the normalized coordinate, L is the grain size

$$z = x/L, \quad (15)$$

the normalized current time is

$$t^* = t/\tau^*, \quad (16)$$

and the normalized current time τ^* is determined by the equation

$$\tau^* = L^2/D, \quad (17)$$

where D is the diffusivity of lithium atoms in the intercalator grain.

Let us write the initial and boundary conditions for Eq. (14). We have

$$\acute{c} \equiv c_0 \quad \text{при } t = 0, \quad (18)$$

on the intercalator grain surface part blocked for lithium atom exchange

$$da/dz = 0 \quad \text{при } z = 0, \quad (19)$$

on the intercalator grain surface in contact with electrolyte grains

$$da/dz = -\lambda j/i_0 = B \quad \text{при } z = 1, \quad (20)$$

where parameter

$$\lambda = (\tilde{n}i_0/Fc^*)(L/D). \quad (21)$$

Let us stress the importance of the presence of parameter $\tilde{n}$. in the expression for λ. This is the average number of electrochemically active faces on the intercalator grain. According to percolation calculations, the number $\tilde{n}$, in the anode varies from 3.55 faces for $g = 0.35$ to 1.91 faces for $g = 0.65$ [19].

Equation (14) seems to allow one to find the sought relationship between concentrations a_s and $\check{c}$. in the intercalator active grain. However, this is not easy insofar as in boundary condition (20) parameter B proves to depend on both the time and the intercalator grain coordinate in the anode active layer. Thus, the processes in the intercalator grain turn out to depend on the potential is being redistributed in the active layer. This is the problem to be solved. It is necessary to elaborate simple algorithms for computations which would allow the working parameters of electrodes to be assessed.

4. THE ROLE OF LITHIUM ATOM DIFFUSIVITY

There are numerous data on the methods of calculation of working parameters of electrodes for lithium ion batteries (e.g., see review [4]). Unfortunately, these methods (see also [20, 21]) are rather complicated and require long machine times. In [22], a simplified procedure was proposed for estimating the electrode working parameters, which makes it possible to quickly obtain final results.

Note the following important factor. The diffusion process in the intercalator active grain and the process of potential redistribution throughout the active layer thickness may be characterized by different characteristic times. The characteristic time of potential redistribution τ is determined by condition (11) and the characteristic time for the diffusion process in an intercalator grain τ^* is determined by condition (17). Let us compare these times. We introduce the parameter

$$\alpha = \tau^*/\tau = L^2Si_0/Dg^*Fc^* = (\zeta i_0/g^*Fc^*)(L/D), \quad (22)$$

where $\zeta = LS$ is the normalized specific contact surface between the electronic and ionic percolation clusters.

In Eq. (22), we assess the factor $\zeta i_0/g^*Fc^*$. Assume that the initial parameters of the anode active mass are the same as in Table 1. Moreover, for definiteness sake, assume that the volume concentration of intercalator

Table 1. Original parameters of the anode active mass

k, Ω^{-1} cm^{-1}	D, cm^2/s	i_o, A/cm^2	L, cm	c^*, g-mol/cm^3	c_0
10^{-3}	10^{-13}	10^{-4}	10^{-5}	3×10^{-2}	0.7

Table 2. Characteristic parameters of the anode active layer

g	g^*	L_{ohm}, cm	I_{ohm}, A/cm^2	τ^*, s	k^*	$\tilde{n}$
0.4	0.348	10^{-3}	1.17×10^{-2}	10^3	0.231	3.35

grains in the active layer $g = 0.4$. Then, it can be shown that $\zeta = 1.167$; the exchange current i_o and the maximum possible lithium concentration in an intercalator grain c^* can be taken from Table 1; the concentration of intercalator active grains g^* can be found in Table 2.

Finally, the factor $\zeta i_0/g^*Fc^* = 10^{-7}$ cm/s. Thus, in place of Eq. (22), we have

$$\alpha = \tau^*/\tau = 10^{-7}(L/D). \quad (23)$$

Now, we begin to vary the grain size L and the diffusivity D of lithium atoms in grains. It is natural to tentatively assume that L values lie in the region $L \geq 10^{-6}$ cm (10 μm) and D values fit the region $D \leq 10^{-8}$ cm^2/s. We shall seek the regions of these parameters in which inequalities $\alpha << 1$ or $\alpha >> 1$ are fulfilled.

Obviously, $\alpha >> 1$ if diffusivity is very low. For $D = 10^{-13}$ cm^2/s and $L = 10^{-5}$ cm, according to Eq. (23) we have $\alpha = 10$. Here, it is also remarkable that as L increases and D decreases, the inequality $\alpha >> 1$ becomes only stronger. Thus, the region of low diffusivities D is defined. In this region, $\alpha >> 1$. Physically, this means that the characteristic time of the diffusion process in intercalator active grains τ^* (Eq. (17)) is much larger than the characteristic time of potential redistribution throughout the active layer thickness τ (Eq. (11)).

It is clear that inequality $\alpha << 1$ should be fulfilled for $D \geq 10^{-12}$ cm^2/s, i.e., in a region which can be reasonably called the region of high diffusivity D. At the same time, here the parameter L is no longer arbitrary because as seen from Eq. (23), the inequality $\alpha << 1$ ceases to work for the infinite increase in L. Thus, L values should be restricted by certain limitations. For example, for $D = 10^{-10}$ cm^2/s, $10^{-6} \leq L \leq 10^{-4}$ cm.

The physical meaning of condition $\alpha << 1$ is that now the characteristic time of the diffusion process in intercalator active grains τ^* is smaller than the characteristic time of potential redistribution throughout the active layer thickness τ. This allows us to sufficiently simplify calculations of working parameters for the electrode active layer.

Thus, we assume that condition $\alpha << 1$ is fulfilled. Then, it can be assumed that electron diffusion in an intercalator grain is the fast process and the potential redistribution in the active layer is the slow process. Hence, system of equations (1)–(21) can be solved in two steps. First, we solve Eq. (14) with boundary conditions (19) and (20). Then we try to find the relationship between concentrations a_s and $\check{c}$ and only after this pass to calculating system of equations (4) and (9).

In [22], it was demonstrated how the approximate solution for the electron concentration redistribution in the intercalator active layer can be found. The final result is as follows:

$$\check{c} = a_s + (\lambda j/i_0) \times \{1/3 - (2/\pi^2)\sum[\exp(-k^2\pi^2 t^*)/k^2]\}, \quad (24)$$

where summation over k in Eq. (24) is carried out from 1 to infinity. Taking into account that when inequality $\alpha << 1$ is fulfilled, we consider only slow processes and have to pass in Eq. (24) from fast time t^* (Eq. (16)) to slow time t^{**} (Eq. (10)). The relationship between these times is evident being given by definition (22)

$$t^* = t^{**}/\alpha. \quad (25)$$

Thus, ultimately, for electrodes with high diffusivities D the following systems of two equations should be used for calculating the working parameters of active layers.

1. For $\alpha \ll 1$,

$$d^2\eta/d\hat{y}^2 = [(1-a_s)^{1/2}a_s^{1/2}]\{e^{\eta} - e^{-\eta}\}, \quad (4)$$

$$d\check{c}/dt^{**} = -[(1-a_s)^{1/2}a_s^{1/2}]\{e^{\eta} - e^{-\eta}\} = -j/i_0, \quad (9)$$

with the additional condition

$$\check{c} = a_s + (\lambda j/i_0) \times \{1/3 - (2/\pi^2)\sum[\exp(-k^2\pi^2 t^{**})/k^2]\}. \quad (24a)$$

The examples of calculations of working parameters for anode active layers in the region of high D values can be found in [22].

Taking into account everything said above, the procedure of calculating the electrode working parameters in the region of low D becomes clear. Here, the slow time is no longer the time characterizing diffusion in the intercalator active layer t^* but the time of potential redistribution in the active layer t^{**}. Furthermore, the calculations of active layer working parameters employ the system of three rather than two equations.

2. For $\alpha \gg 1$,

$$d^2\eta/d\hat{y}^2 = [(1-a_s)^{1/2}a_s^{1/2}]\{e^{\eta} - e^{-\eta}\}, \quad (4)$$

$$d\check{c}/dt^* = -\alpha[(1-a_s)^{1/2}a_s^{1/2}]\{e^{\eta} - e^{-\eta}\} = -\alpha j/i_0, \quad (9a)$$

$$da/dt^* = d^2a/dz^2. \quad (14)$$

It should be noted that in Eq. (9), the fast time t^{**} was changed for the slow time t^*.

The problem for the case of $\alpha >> 1$ has become more complicated because, first of all, now we have to solve the system of three rather than two equations and, second, one of boundary conditions for Eq. (14) depends on time. Parameter B in Eq. (20) stops to be constant. Below, we discuss how one can estimate the working parameters of the anode active layer by using the system of equations (4), (9a), and (14).

5. ALGORITHMS OF CALCULATIONS IN THE REGION OF LOW DIFFUSIVITY VALUES

A numerical study of the spatial-temporal distribution of normalized polarization in the electrode active layer η (y, t) and the average concentration of lithium atoms in intercalator grains $\check{c}$ (y, t) was carried out in terms of a model analogous to that shown in [3, 20]. The active layer of the anode was considered as a continuous medium in which the normalized polarization is a continuous function determined by solution of Eq. (4). This medium contains intercalator grains which are assumed to be discrete objects (of a small but finite size) in which lithium atoms diffuse to the grain boundary where the electrochemical process takes place. In each grain, the diffusion process is described by Eq. (14), where the current density $j(t^*, y)$ is determined by the concentration a_s (t^*, y) of lithium atoms near the electrochemically active grain surface and depends on polarization η (y) in the grain location place.

Such a "continuous-discrete" description is conventionally used as the basic model when studying many characteristics of lithium-ion batteries, particularly, the temperature effects associated with heat transfer [23], simulations of cycling life when considering the mechanism of continuously varying capacitance [24, 25].

To solve nonlinear differential equations both common and in partial derivatives, it is practice to use "grid" methods of numerical calculations such as the method of finite elements [2], method of finite differences [27, 28], Monte-Carlo method [29]. They are based on the idea of discretization of the problem and the transfer from partial derivatives involved in equations to approximate difference ratios. The original differential equation is substituted by a system of algebraic equations referred to as the difference scheme. By solving this problem it is possible to find the grid function values in grid points, which are assumed to be approximately equal to the sought function.

The accuracy of these methods is determined by the number of grid points. However, the larger the number of points (i.e., the smaller spatial and temporal intervals), the larger the machine memory and time we need. This is why it was impossible to use some of these methods in the present study, because for each point of the grid built for solving Eq. (4), we had to solve nonstationary Eq. (14) and introduce additional spatial grids.

In this study, the numerical solution of system of equation (4), (9a), and (14) was carried out by a complex method, namely, Eq. (4) was solved by the method of finite differences [30], Eq. (9a) was integrated by the method of Euler-Cauchy [31], and the solution of Eq. (14) was sought analytically with the use of the method of "pseudo-stationary states" [32, 33].

Within the framework of this approach, the anodic active layer was divided into N layers. The layer boundaries are the spatial grid "points" with coordinates $y_i = \Delta\frac{i}{N}$, in which the normalized polarization $\eta(y_i, t_k^*)$ in a fixed moment can be found by solving Eq. (4).

The right side of this equation contains the current density on the surface of the grain localized in the corresponding grid point. The current density is determined by the concentration $a_s(y, t^*)$ of lithium atoms near the electrochemically active surface of this grain. This concentration can be found by solving Eq. (14a) with nonstationary boundary conditions.

The algorithm of solution of the problem posed is as follows. First of all, a sufficiently small time step Δt^* is chosen such that the current density can be assumed constant in the interval from t_k^* to $t_k^* + \Delta t^*$. In the first (initial) stage, we determine the distribution of the normalized polarization $\eta(y_i, 0)$ in moment $t^* = 0$ by solving the equation

$$\frac{d^2\eta(y, 0)}{dy^2} = \sqrt{(1 - c_0)c_0} \times 2\sinh\{\eta(y, 0)\}$$

$$/a_s(y, 0) = c_0/.$$

Assuming that during the time interval Δt^*, the current density at the boundary of each grain remains unchanged, i.e.,

$$J_i(t^*) = J_i(0) = \lambda\sqrt{(1 - c_0)c_0}\,2\sinh\{\eta(y_i, 0)\},$$

we find the concentration distribution of lithium atoms in grains in the moment $t_k^* = 0 + \Delta t^*$ by solving analytically Eq. (14) (the derivation is shown below)

$$a_i(t_1^*, z) = c_0 + \left(\frac{1 - 3z^2}{6} - \Delta t^*\right)J_i(0)$$

$$+ J_i(0)\frac{2}{\pi^2}\sum_{n=1}^{\infty}\frac{(-1)^n\cos(\pi n z)}{n^2}\exp(-\pi^2 n^2\Delta t^*).$$

Hence, to this moment, the lithium atom concentration at the grain boundary ($z = 1$) becomes equal to

$$a_{s,i}(t_1^*) = c_0 - \left(\frac{1}{3} + \Delta t^*\right) J_i(0) + J_i(0)\frac{2}{\pi^2}\sum_{n=1}^{\infty}\frac{\exp(-\pi^2 n^2 \Delta t^*)}{n^2}.$$

The further calculations are analogous. In each time step, we assume that the current density is determined by values $a_{s,i}(t_{k-1}^*)$ and $\eta(y_i, t_{k-1}^*)$ in the previous moment. Then, in moment $t_k^* = k\Delta t^*$, we calculate the lithium atom concentration on the grain surface by using the equality

$$a_{s,i}(t_k^*) = \int_0^1 a(t_{k-1}^*)dx - \left(\frac{1}{3} + \Delta t^*\right) J_i(t_{k-1}^*) + J_i(t_{k-1}^*)\frac{2}{\pi^2}\sum_{n=1}^{\infty}\frac{\exp(-\pi^2 n^2 \Delta t^*)}{n^2} + 2\sum_{n=1}^{\infty}(-1)^n \left\{\int_0^1 \{a(t_{k-1}^*, x)\cos(\pi n x)\}dx\right\}\exp(-\pi^2 n^2 \Delta t^*),$$

where

$$J_i(t_{k-1}^*) = \lambda\sqrt{[1 - a_{s,i}(t_{k-1}^*)]a_{s,i}(t_{k-1}^*)} \times 2\sinh\{\eta(y_i, t_{k-1}^*)\},$$

$$a(t_{k-1}^*, y_i) = \int_0^1 a(t_{k-2}^*, x)dx + \left[\frac{1 - z^2}{6} - \Delta t^*\right] J_i(t_{k-2}^*) + 2\sum_{n=1}^{\infty}\left\{\frac{(-1)^n}{n^2\pi^2} J_i(t_{k-2}^*) + \int_0^1 a(t_{k-2}^*, x)\cos(\pi n x)dx\right\} \times \cos(\pi n z)e^{-\pi^2 n^2 \Delta t^*}.$$

Then, we solve Eq. (4) in the following form:

$$\frac{d^2\eta(y, t_k^*)}{dy^2} = \sqrt{(1 - a_s(t_k^*, y))a_s(t_k^*, y)} \times 2\sinh\{\eta(y, t_k^*)\}.$$

The cycle of calculations is finished when the surface concentration of lithium atoms on the active layer boundary reaches a certain permissible minimum. As this minimum, we have chosen the value $\min a_s = 0.01$. It deserves mention that summation of series was stopped at the term with the relative contribution of $<10^{-6}$. In this case, the time interval Δt^* was chosen such that when this interval was halved, the relative error of final values $a_s(t^*, y = 0)$ did not exceed 0.001.

The averaged concentration of lithium ions in a graphite grain was calculated by numerical integration of Eq. (9a) by the trapezium method [30]

$$\check{c}(t_k^*, y_i) = c_0 - \frac{\Delta t^*}{2}\sum_{k=1}^{k_{max}}[\hat{j}_i(t_k^*) - \hat{j}_i(t_{k-1}^*)],$$

where

$$\hat{j}_i(t_k^*) = \alpha\sqrt{(1 - a_s(t_k^*, y_i))a_s(t_k^*, y_i)} \times 2\sinh\{\eta(y_i, t_k^*)\}.$$

Problem of Lithium Atom Distribution in Graphite Grains

Let us consider the diffusion of lithium atoms in an individual active graphite grain the position of which in the anode active layer is determined by coordinate y_i. Due to the small size, we can assume that within the grain, the normalized polarization is uniform and equal to $\eta = \eta(t, y_i)$, i.e., to its value in a point of spatial grid representing the anode model.

The flow density through the grain boundary and the distribution of lithium atom concentration in the grain are interrelated nonstationary values. Hence, to simplify this method, we use the method of "pseudo-stationary states". We assume that in a certain sufficiently small time interval Δt, the flow of atoms can be assumed to be stationary; moreover, its numerical value is determined by the distribution of atoms throughout the grain in the previous moments. Then, the problem of diffusion of atoms in the grain in the interval $t_k^* \le t^* \le t_{k+1}^*$ reduces to solving the equation

$$\frac{\partial a_i(t, z)}{\partial t} = \frac{\partial^2 a_i(t, z)}{\partial z^2} \quad 0 \le t \le \Delta t^*, \quad 0 \le z \le 1 \qquad \text{(A)}$$

with boundary conditions

$$\frac{\partial a_i(t, 0)}{\partial z} = 0 \quad \text{и} \quad \frac{\partial a_i(t, 1)}{\partial z} = -J_i(t_k^*), \qquad \text{(B)}$$

and the initial condition

$$a_i(0, z) = a_i(t_k^*, z),$$

where

$$t = t^* - t_k^*,$$

$$J_i(t_k^*) = \lambda 2\sinh\{\eta(t_k^*, y_i)\}\sqrt{a_s(t_k^*, y_i)[1 - a_s(t_k^*, y_i)]}.$$

We represent the sought function (subscript i is omitted) as a sum

$$a(t, z) = v(t, z) + \psi(t, z).$$

Function $\psi(t, z)$ is required to fulfill boundary conditions (B). For this to be true, this function should be represented as follows:

$$\psi(t, z) = -J(t_k^*)\frac{z^2}{2}.$$

Then, for function $v(t, z)$, we obtain the following nonuniform equation

$$\frac{\partial v(t, z)}{\partial t} = \frac{\partial^2 v(t, z)}{\partial z^2} - J(t_k^*) \quad \text{(C)}$$

with boundary conditions

$$\frac{\partial v(t, 0)}{\partial z} = 0 \quad \text{и} \quad \frac{\partial v(t, 1)}{\partial z} = 0 \quad \text{(D)}$$

and the initial condition

$$v(0, z) = a(t_k^*, z) + J(t_k^*)\frac{z^2}{2}. \quad \text{(E)}$$

Now, we seek the solution of Eq. (C) according to the Fourier method in the form

$$v(t, z) = \frac{v_0(t)}{2} + \sum_{n=1}^{\infty} v_n(t)X_n(z). \quad \text{(F)}$$

Functions $X_n(z) = \cos(\pi n z)$, $(n = 0, 1, 2 \ldots)$ represent the solution of the problem of Sturm–Liouville

$$\frac{d^2}{dz^2}X(z) + \lambda^2 X(z) = 0,$$

$$\frac{dX}{dz} = 0 \text{ at } x = 0 \text{ and } \frac{dX}{dz} = 0 \text{ at } x = 1.$$

Substitution of Eq. (F) into Eq. (C) gives the equality

$$\frac{\partial}{\partial t}\frac{v_0(t)}{2} + \sum_{n=1}^{\infty}\frac{\partial}{\partial t}v_n(t)X_n(z) = -\sum_{n=1}^{\infty} v_n(t)\lambda_n^2 X_n(z) - J(t_k^*).$$

By magnifying both sides of this equality by $X_n(z)$ and integrating over z in the interval from 0 to 1, we obtain the system of common differential equations with respect to variable t

$$\frac{dv_0(t)}{dt} = -2J(t_k^*),$$

$$\frac{dv_n(t)}{dt} = -\lambda_n^2 v_n(t).$$

The solution of this system represents the functions

$$v_0(t) = v_0(0) - 2J(t_k^*)t$$

$$\text{and } v_n(t) = v_n(0)\exp(-\pi^2 n^2 t).$$

Let us take into account the initial condition (E)

$$\frac{v_0(0)}{2} + \sum_{n=1}^{\infty} v_n(0)X_n(z) = a(t_k^*, z) + J(t_k^*)\frac{z^2}{2}.$$

By expanding the right side in the Fourier series with respect to eigenfunctions $X_n(z)$ with norm $\|A\| = 1/2$, we have

$$v_0(0) = 2\int_0^1 a(t_k^*, z)dz + \frac{1}{3}J(t_k^*),$$

$$v_n(0) = 2\int_0^1 \left(a(t_k^*, z) + J(t_k^*)\frac{z^2}{2}\right)\cos(\pi n z)dz$$

$$= 2\int_0^1 a(t_k^*, z)\cos(\pi n z)dz + \frac{2(-1)^n}{\pi^2 n^2}J(t_k^*).$$

Thus, the general solution of Eq. (A) has the form

$$a_i(t_{k+1}^*, z) = \int_0^1 a_i(t_k^*, x)dx + \left(\frac{1-3z^2}{6} - t\right)J_i(t_k^*) + 2\sum_{n=1}^{\infty}\left\{\frac{(-1)^n J_i(t_k^*)}{n^2\pi^2} + \int_0^1 a_i(t_k^*, x)\cos(\pi n x)dx\right\} \times \cos(\pi n z)e^{-\pi^2 n^2 \Delta t^*}. \quad \text{(G)}$$

On the electrochemically active grain boundary ($z = 1$), the lithium concentration is determined by the expression

$$a_{*i,\,S}(t) = \int_0^1 a_i(t_k^*, x)dx - \left(\frac{1}{3} + t\right)J_i(t_k^*) + 2\sum_{n=1}^{\infty}\left\{\frac{J_i(t_k^*)}{n^2\pi^2} + (-1)^n\int_0^1 a_i(t_k^*, x)\cos(\pi n x)dx\right\} \times \exp(-\pi^2 n^2 t). \quad \text{(H)}$$

6. DETERMINATION OF WORKING PARAMETERS OF ANODE FOR A >> 1

Now, we can calculate the working parameters of the anode active layer with characteristics shown in Tables 1 and 2. Parameter $\alpha = 11.58$; hence, the calculations were carried out by using the system of equations (4), (9a), and (14). The procedure of calculations is described in the previous section. The discharge current density $I = 1$ mA/cm^2.

Here we describe the results of calculations. Figure 1a shows how the concentration distribution of lithium atoms on the electrochemically active surface of intercalator grains varies in time along the anode active layer thickness ($\Delta = 1$ mm). The discharge

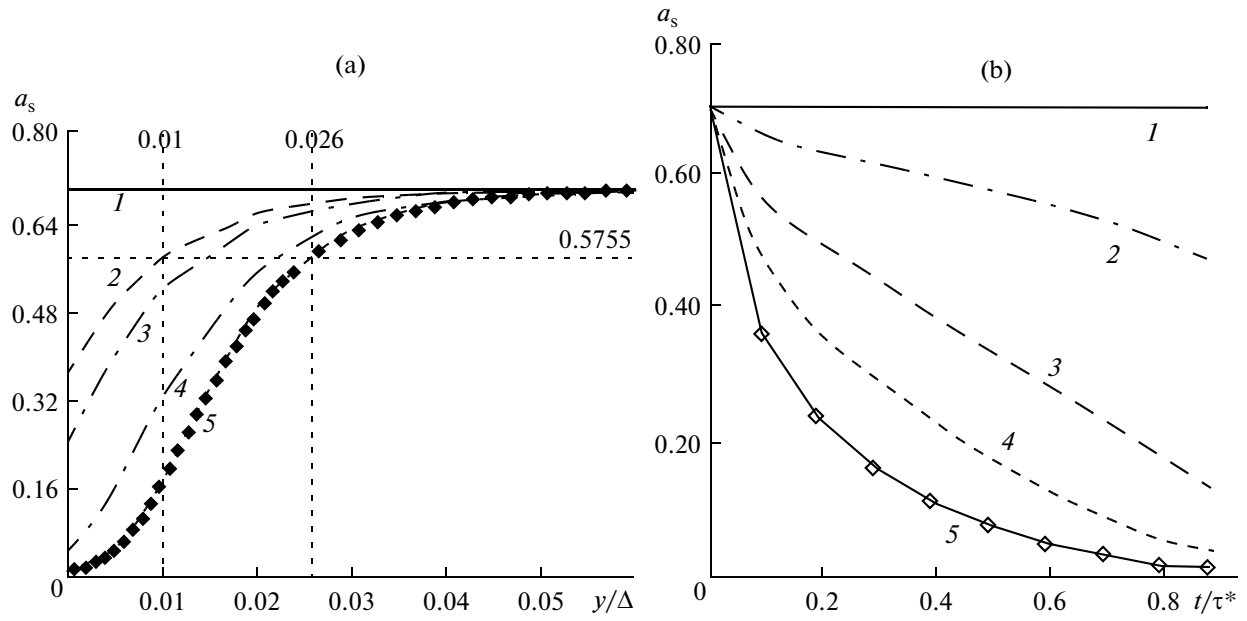

Fig. 1. Time variations of the lithium atom concentration distribution along the active layer thicknessr on electrochemically active surface of intercalator grains localized on the anode of a lithium-ion battery. y/Δ is the normalized active layer thickness, t/τ^* is the normalized discharge time. (a) t/τ^* (*1*) 0, (*2*) 0.09, (*3*) 0.19, (*4*) 0.59, (*5*) 0.88. (b) y/Δ: (*1*) 1.0, (*2*) 0.03, (*3*) 0.01, (*4*) 0.005, (*5*) 0.0. $D = 10^{-13}$ cm^2/s, $L = 10^{-5}$ cm, $I = 1$ mA/cm^2, $\Delta = 1$ mm.

stopped when the concentration of lithium atoms a_s at the active layer/interelectrode space interface in intercalator active grains dropped to 0.01. The discharge time was 880 s. Figure 1b shows how the concentration of lithium atoms a_s varies in time in different layers in intercalator active grains of the anode active layer.

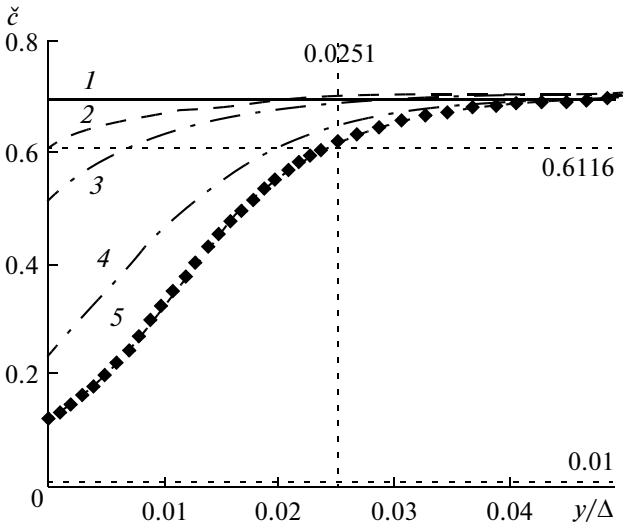

Fig. 2. Time variations of the distribution of average concentration of lithium atoms in intercalator active grains along the thickness of the active layer on the anode of a lithium-ion battery. y/Δ is the normalized active layer thickness. The normalized discharge time t/τ^*: (*1*) 0, (*2*) 0.09, (*3*) 0.19, (*4*) 0.59, (*5*) 0.88. $D = 10^{-13}$ cm^2/s, $L = 10^{-5}$ cm, $I = 1$ mA/cm^2, $\Delta = 1$ mm.

It is helpful to compare the data in Fig. 1 and Fig. 2. Obviously, the complete depletion of intercalator active grains at the anode active layer/interelectrode space interface is never reached. In the moment of discharge cessation (curve *5* in Fig. 2), the average concentration of lithium atoms still differs from zero.

Figure 3 shows time variations of the potential distribution along the active layer thickness on the anode of a lithium-ion battery. Here, t/τ^* is the normalized discharge time, y/Δ is the normalized active layer thickness. (a) y/Δ: (*1*) 1.0, (*2*) 0.03, (*3*) 0.01, (*4*) 0.005, (*5*) 0.0; (b) t/τ^*: (*1*) 0, (*2*) 0.09, (*3*) 0.19, (*4*) 0.59, (*5*) 0.88.

Figure 4 shows how the lithium atom concentration varies along the active grain thickness in time for an intercalator active grain located at the anode active layer/interelectrode space interface. Here, x/L is the normalized intercalator grain thickness. We are convinced once more that if on the front side of a grain where the electrochemical process occurs, the lithium atom concentration is virtually zero then on its back side the lithium atom concentration still differs from zero so that on the whole, the intercalator grain is only partly depleted of lithium atoms at the discharge.

In above calculations we assumed that the discharge current density $I = 1$ mA/cm^2. A question arises of how an increase or a decrease in the discharge current can affect the anode working parameters. We carried out the corresponding calculations for three discharge current values: 10, 1, and 0.1 mA/cm^2. Fig-

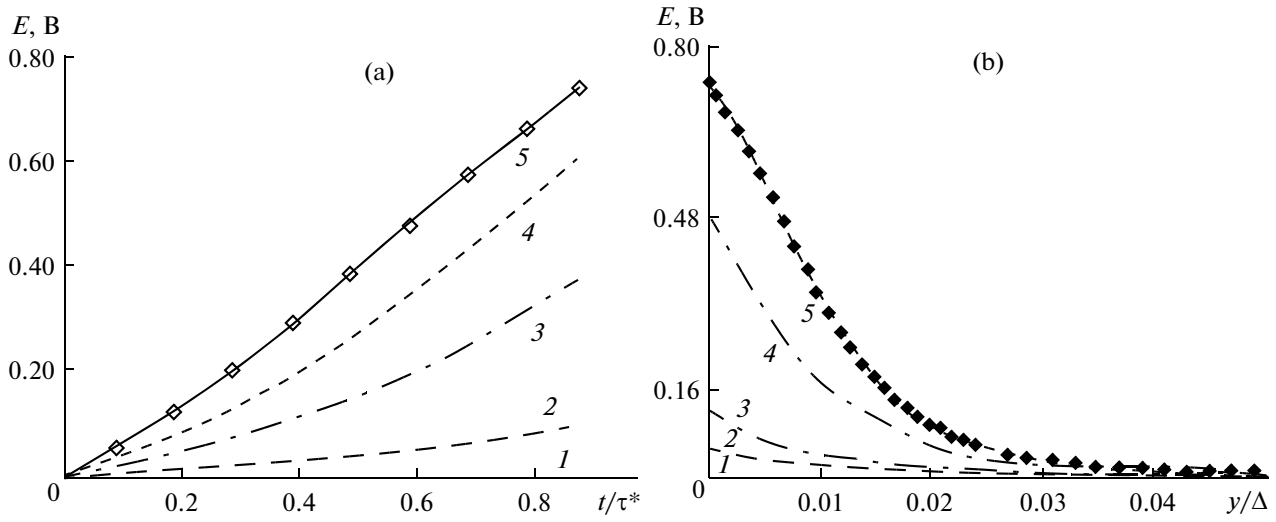

Fig. 3. Time variations of the potential distribution along the anode active layer in a lithium-ion battery, t/τ^* is the normalized discharge time, y/Δ is the normalized active layer thickness, (a) y/Δ: (*1*) 1.0, (*2*) 0.03, (*3*) 0.01, (*4*) 0.005, (*5*) 0.0. (b) t/τ^*: (*1*) 0, (*2*) 0.09, (*3*) 0.19, (*4*) 0.59, (*5*) 0.88. $D = 10^{-13}$ cm^2/s, $L = 10^{-5}$ cm, $I = 1$ mA/cm^2, $\Delta = 1$ mm.

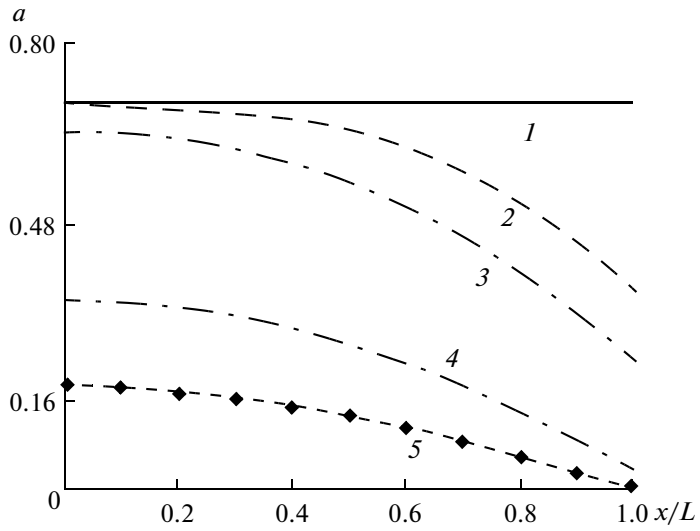

Fig. 4. Time variations of lithium atom concentration distribution along the intercalator active grain at the active layer/interelectrode space interface. x/L is the normalized intercalator grain thickness. Normalized discharge time t/τ^*: (*1*) 0, (*2*) 0.09, (*3*) 0.19, (*4*) 0.59, (*5*) 0.88. $D = 10^{-13}$ cm^2/s, $L = 10^{-5}$ cm, $I = 1$ mA/cm^2.

ures 5–7 show the results of these calculations. For $I =$ 10 mA/cm^2, in the moment the discharge stops, the concentration differs little from initial one (Fig. 5, curve *1*) and the potential at the anode active layer/interelectrode space interface is very low (Fig. 6, curve *1*); hence, the process of active layer depletion of lithium atoms at the anode active layer/interelectrode space interface is weak (Fig. 7, curve *1*).

For the discharge current $I = 1$ mA/cm^2, the situation cardinally changes. There is noticeable depletion of intercalator active grains in a layer adjusting the anode active layer/interelectrode space interface (Fig. 5, curve *2*). The anode potential at the active layer/ interelectrode space interface considerably increases (Fig. 6, curve *2*) and the depletion of intercalator active grains at the anode active layer/interelectrode space interface becomes noticeable (Fig. 7, curve *2*).

As evident from curves *3* in Figs. 5 and 7, the virtually complete extraction of lithium atoms from intercalator active grains can be achieved by reducing the current density down to $I = 0.1$ mA/cm^2. Then, the anode potential at the interface active layer/interelectrode space (Fig. 6, curve *3*) increases up to 1 V.

Table 3 shows working parameters of the lithium-ion battery anode for all three values of discharge cur-

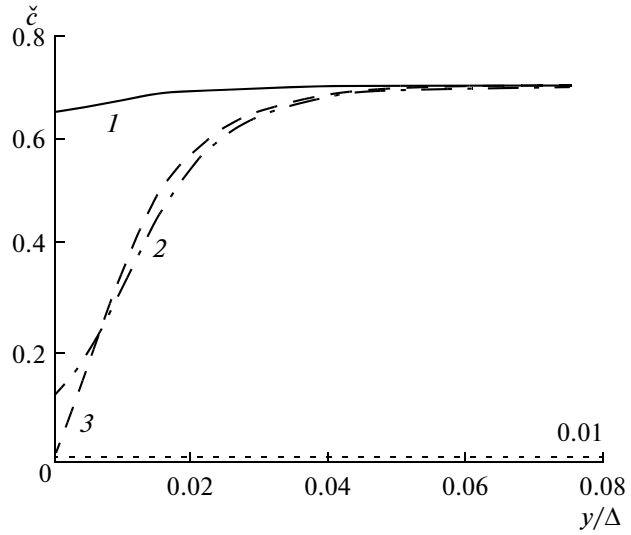

Fig. 5. Final distributions of the average concentration of lithium ions in intercalator active grains along the active layer thickness on the anode of a lithium-ion battery. y/Δ is the normalized active layer thickness. Discharge current density I, mA/cm^2: (*1*) 10, (*2*) 1, (*3*) 0.1. $D = 10^{-13}$ cm^2/s, $L = 10^{-5}$ cm, $\Delta = 1$ mm.

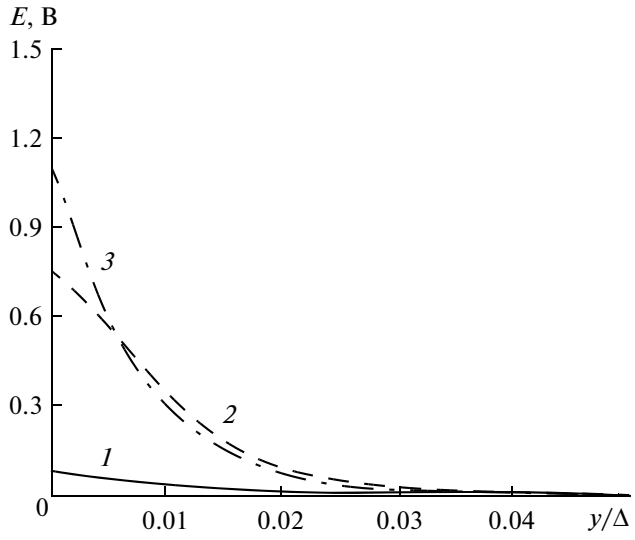

Fig. 6. Final potential distributions along the thickness of the active layer of the anode of a lithium-ion battery. y/Δ is the normalized active layer thickness. Discharge current density I, mA/cm^2: (*1*) 10, (*2*) 1, (*3*) 0.1. $D = 10^{-13}$ cm^2/s, $L = 10^{-5}$ cm, $\Delta = 1$ mm.

rent density. The optimal active layer thickness (the second column in Table 3, the procedure of its determination can be found in [1]) is low, ca. 23–26 μm. This is associated with the fact that the characteristic ohmic length (Eq. (5)) is proportional to square root of the grain size in the active layer $L_{ohm} \sim L^{1/2}$ and the value of L was assumed to be small, i.e., $L = 0.1$ μm (data of Table 1).

The procedure of estimating the discharge time ($t^{***}\tau$, s, the 3rd column in Table 1) can also be found in [1]. The specific capacitance of the anode was assessed according formula $C = It^{***}\tau$, C/cm^2. As the discharge current decreases, the anode capacitance (the 4th column in Table 3) tends to its limiting value.

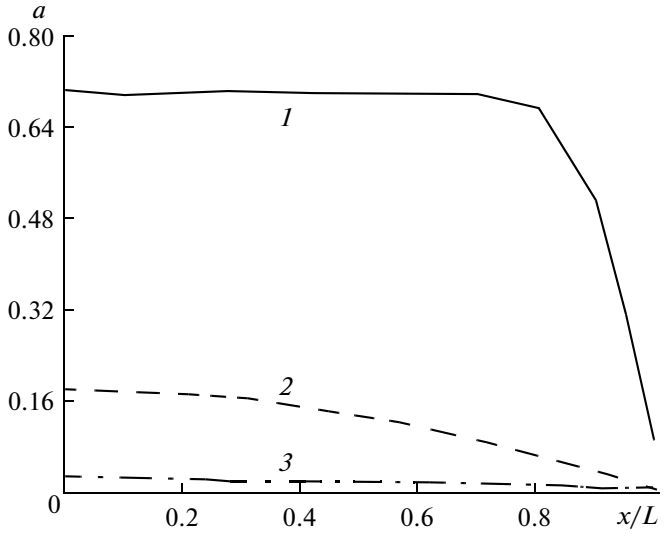

Fig. 7. Final distributions of lithium atom concentration along the thickness of the intercalator active grain at the interface anodic active layer/interelectrode space. x/L is normalized thickness of an intercalator grain. Discharge current density I, mA/cm^2: (*1*) 10, (*2*) 1, (*3*) 0.1. $D = 10^{-13}$ cm^2/s, $L = 10^{-5}$ cm.

CONCLUSION

The structure and characteristics of active layers on electrodes of lithium-ion batteries operating in the galvanostatic discharge mode was simulated. Attention was focused on the complete mathematic description of processes in active layers of electrodes.

The central problem of the theory of such systems lies in the fact that simultaneously two interconnected process take place in space and time, namely, the diffusion of lithium atoms in intercalator grains and the potential redistribution along the electrode active layer induced by ohmic limitations.

Numerous publications were devoted to methods of calculating the parameters of active layers on lithium-ion battery electrodes. Unfortunately, they are complicated and require long machine times. In the present study, we put forward a simplified procedure for calculating working parameters of electrodes, which allows the final results to be obtained sufficiently easily and quickly.

This new approach to the central problem is based on comparing the characteristic times of two main processes in electrodes. Here, the decisive role is played by the diffusivity of lithium atoms in intercala-

tor grains. Two regions of lithium atom diffusivity values can be singled out, i.e., high and low diffusivities.

Algorithms of calculation of the complete system of equations for the most complicated case, namely, for active layers of arbitrary thickness with low lithium atom diffusivities, have been developed.

The calculations of electrode (anode) working parameters were carried out for active layers of arbitrary thickness and low diffusivity values. The optimal values of active layer thickness, discharge time, specific capacitance, and final potential at the anode active layer/inerelectrode space interface were estimated. The found parameters are by and large consistent with experimental data.

DESIGNATIONS FOR PARAMETERS OF THE ANODE ACTIVE LAYER WITHIN LITHIUM ION BATTERY

External parameters

t is the current time of anode discharge

$t^* = t/\tau^*$ is the normalized current time of extraction of lithium ions from an intercalator active grain

τ^* is the characteristic time of extraction of lithium atoms from an intercalator active grain

$t^{**} = t/\tau$ is the normalized current time for the anode discharge (active layer as a whole)

τ is characteristic time of anode discharge (active layer as a whole)

t^{***} is the normalized time of anode discharge

C, C/cm^2 is specific capacitance of the anode

R is the gas constant

$T = 293$ K is the anode working temperature

Δ is the anode active layer thickness used in calculations

$\tilde{n}$ is the average number of electrochemically active faces of an intercalator active grain

Parameters of electrochemical kinetics

$F = 9.65 \times 10^4$ C/mol is the Faraday number

I, A/cm^2 is the current density of anode discharge

j, A/cm^2 is the current density of the electrochemical reaction

i_0 is the exchange current

η is the normalized polarization

ψ is the normalized anodic potential

E is the anodic potential

U is the open-circuit potential of an intercalator grain

L_{ohm} is the characteristic ohmic length

I_{ohm}, A/cm^2 is the characteristic ohmic current

y is the anode active layer coordinate

Table 3. Working parameters of the anode

I, mA/cm^2	Δ^*, μm	$t^{***}\tau$, s	C, C/cm^2	E^*, V
10	24	5.4	0.054	0.07
1	26	880	0.88	0.73
0.1	23.5	8500	0.85	1.07

$\hat{y} = y/L_{ohm}$ is the normalized coordinate in the anode active layer

Parameters of the anode active layer structure

g is the volume concentration (ratio) of intercalator grains

g^* ($g^* < g$) is the ratio of intercalator active grains

L is the size of intercalator and electrolyte grains

S, cm^{-1} is the specific contact surface between electronic and ionic percolation clusters

$\zeta = SL$ is the normalized specific contact surface between electronic and ionic percolation clusters

Parameters of the intercalator grain structure

c is the concentration of lithium atoms averaged over the intercalator grain volume

c^* is the maximum possible lithium concentration in an intercalator grain

$\check{c} = c/c^*$ is the normalized concentration of lithium atoms averaged over the intercalator grain volume

$\check{c} = c_0$ is the initial saturation of intercalator grains with lithium atoms

Parameters determining diffusion processes in an intercalator grain

a is the normalized concentration of lithium atoms in the intercalator active grain

a_s is the normalized concentration of lithium atoms at the electrochemically active surface of an inercalator grain

$z = x/L$ is the normalized coordinate in the intercalator grain

$\alpha = \tau^*/\tau$ is a constant determining the mode of lithium atom extraction from intercalator grains

B is a constant determining the mode of lithium atom extraction from intercalator grains

Parameters determining the processes of mass and electro transfer

D is the diffusivity of lithium atoms in intercalator grains

k is the specific conductivity of electrolyte

k^* is the conductivity (dimensionless) of lithium ions in a percolation ionic cluster

kk^* is the specific conductivity of the anode active layer

REFERENCES

1. Chirkov, Yu.G., Rostokinv, V.I., and Skundin, A.M., *Russ. J. Electrochem.*, 2011, vol. 47, p. 59.
2. Chirkov, Yu.G., Rostokin, V.I., and Skundin, A.M., *Russ. J. Electrochem.*, 2011, vol. 47, p. 77.
3. Fuller, T.F., Doyle, M., and Newman, J., *J. Electrochem. Soc.*, 1994, vol. 141, p. 1.
4. Zhang, Q. and White, R.E., *J. Power Sources*, 2008, vol. 179, p. 793.
5. Churikov, A.V., *Russ. J. Electrochem.*, 2002, vol. 38, p. 103.
6. Huggins, R.A., *J. Power Sources*, 1999, vol. 81, p. 13.
7. Zang, T., Fu, L.J., Gao, J., Wu, Y.P., Holze, R., and Wu, H.Q., *J. Power Sources*, 2007, vol. 174, p. 770.
8. Hamon, Y., Brouse, T., Jousse, F., Topart, P., Buvat, P., and Schleich, D.M., *J. Power Sources*, 2001, vol. 97, p. 185.
9. Liu, Y., Mi, C., and Su, L., Zhang, X., *Electrochim. Acta*, 2008, vol. 53, p. 2507.
10. Liu, Y. and Zhang, X., *Electrochim. Acta*, 2009, vol. 54, p. 4180.
11. Kulova, T.L., Skundin, A.M., Pleskov, Yu.V., Kon'kov, O.I., Terukov, E.I., and Trapeznikova, I.N., *Fiz. Tekh. Poluprovodn. (S.-Peterburg)*, 2006, vol. 40, p. 473.
12. Kulova, T.L., Skundin, A.M., Pleskov, Yu.V., Terukov, E.I., and Kon'kov, O.I., *Russ. J. Electrochem.*, 2006, vol. 42, p. 363.
13. Kulova, T.L., Skundin, A.M., Pleskov, Yu.V., Terukov, E.I., and Kon'kov, O.I., *Russ. J. Electrochem.*, 2006, vol. 42, p. 708.
14. Kulova, T.L., Skundin, F.M., Pleskov, Yu.V., Terukov, E.I., and Kon'kov, O.I., *J. Electroanal. Chem.*, 2007, vol. 600, p. 217.
15. Shenuoda, A.Y. and Hua Kun Liu, *J. Power Sources*, 2008, vol. 185, p. 1386.
16. Makaev, S.V., Ivanov, V.K, Kulova, T.L., Polezhaeva, O.S., Brylev, O.A., Skundin, A.M., and Tret'yakov, Yu.D., *Russ. J. Inorg. Chem.*, 2010, vol. 55, p. 991.
17. Sharma, Y., Sharma, N., Subba Rao, G.V., and Chowdari, B.V.R., *J. Power Sources*, 2009, vol. 192, p. 627.
18. Kulova, T.L., Skundin, A.M., Trubnikova, L.V., and Maizelis, A.A., *Vopr. Khim. Khim. Tekhnol.*, 2011, no. 4, p. 303.
19. Chirkov, Yu.G., Rostokin, V.I., and Skundin, A.M., *Russ. J. Electrochem.*, 2011, vol. 47, p. 288.
20. Doyle, M. and Newman, J., *J. Electrochem. Soc.*, 1993, vol. 140, p. 1526.
21. Doyle, M., Newman, J., Gozdz, A.S., Schmutz, C.N., and Tarascon, J.-M., *J. Electrochem. Soc.*, 1996, vol. 143, p. 1890.
22. Chirkov, Yu.G., Rostokin, V.I., and Skundin, A.M., *Russ. J. Electrochem.*, 2011, vol. 47, p. 768.
23. Gomadam, P.M., Weidner, J.W., Doudal, R.A., and White, R.E., *J. Power Sources*, 2002, vol. 110, p. 267.
24. Ramadass, P., Haran, B., White, R.E., and Popov, B.N., *J. Power Sources*, 2003, vol. 123, p. 230.
25. Sigha, G., Popov, B.N., and White, R.E., *J. Electrochem. Soc.*, 2004, vol. 151, p. A1104.
26. Segerlind, L., *Primenenie metoda konechnykh elementov* (Application of the Finite Element Technique), Moscow, 1979.
27. Strikwerda, J., *Finite Difference Schemes and Partial Differential Equations*, Wadsworth and Brooks/Cole, 1989.
28. Samarskii, A.A. and Vabishchevich, P.N., *Vychislitel'naya teploperedacha* (Heat Transfer Computations), Moscow: Knizhnyi dom LIBROKOM, 2009.
29. Elepov, B.C., Kronberg, A.A., Mikhailov, G.A., and Sabel'fel'd, K.K., *Reshenie kraevykh zadach metodom Monte-Karlo* (Solving Boundary problems by the Monte-Carlo Method), Novosibirsk: Nauka, 1980.
30. Bakhvalov, N.V., Zhidkov, N.P., and Kobel'kov, G.M., *Chislennye metody* (Numerical Methods), Moscow: Laboratoriya Bazovykh Znanii, 2002.
31. Smirnov, V.I., *Kurs vysshei matematiki* (Higher Mathematics Course), Moscow: Nauka, 1974, vol. 2.
32. Ölçer, N.Y., *Int. J. Heat Mass Transfer*, 1964, vol. 7, p. 307.
33. Ölçer, N.J., *Int. J. Heat Mass Transfer*, 1965, vol. 8, p. 529.

Translated by T. Safonova

SPELL: 1. ok